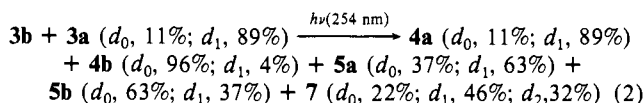


content),<sup>11</sup> was irradiated in benzene for 5 h; the conversions of **3a,b** were found by GLC analysis to be 87% and 76%, respectively. The deuterium contents of the products were determined as shown in eq 2.<sup>11</sup> Expectedly, the observed  $d_0:d_1:d_2$  ratio in bibenzyl (**7**)



is compared with a calculated ratio based on the random encounter of the generated benzyl radicals,<sup>12</sup>  $d_0:d_1:d_2 = 30:50:20$ . Whereas cross products were produced in significant amounts in **5a** and **5b**, no scrambling of deuterium was observed in **4a** and **4b** as well as in recovered **3a** and **3b** within experimental errors.

Therefore, it can be concluded that the formation **4** occurred only in the solvent cage, while **5** arises as both cage and escaped products. These results imply that **10** is formed in the cage as a transient species during the acyloxy migration.

Further insight into the mechanism of the free radical acyloxy migration was given by ESR. Thus, the superimposed ESR spectra of two radical species, **9b** and **11b**, were observed between -134 and -80 °C,<sup>13</sup> when a mixture of (acetoxymethyl)dimethylsilane, di-*tert*-butyl peroxide, and cyclopropane was photolyzed in an ESR cavity. The relative signal intensity of **11b** to **9b** increased with increasing temperature. It is worthy of noting that the rearrangement from **9b** to **11b** is observed even at very low temperatures compared with the corresponding acyloxy migration from carbon to carbon, which are usually studied at around 80 °C.<sup>10</sup> The activation energy for the rearrangement from **9b** to **11b** is suggested to be much lower than that for the 1,2 (C → C) acyloxy migration.<sup>14,15</sup>

No signal due to **10b** was detected by ESR in the temperature range studied probably because of its short lifetime. The success of detecting **10** as **4** in the present case may be a result of the concurrent generation of an effective radical trap such as **8** in the vicinity of **10**.<sup>17</sup> Further works are in progress.

**Acknowledgment.** The work is supported in part by the Ministry of Education, Science, and Culture (Grant-in-Aid for Scientific Research 59470013). We thank Toshiba Silicone Co., Ltd., for gifts of chlorosilanes.

(11) The deuterium contents in starting materials and products were all determined by mass spectral analysis.

(12) The small discrepancy between the observed and calculated ratios may be caused by the difference of the cage efficiency between **3a** and **3b**. Assuming that the ratio between benzyl and benzyl-*d*<sub>1</sub> radicals escaping from the solvent cage is reflected in the  $d_0:d_1:d_2$  ratio observed in **7**, **5a** and **5b** generated in the cage are estimated as 24% and 33% of the total, respectively.

(13) The hyperfine splitting constants (hfs) of these radicals were determined as follows at -134 °C. **9b**: 3.25 (2 H), 6.50 G (6 H). **11b**: 21.3 (2 H), 0.69 G (6 H). The triplet hfs of **9b** increased with increasing temperature ( $da/dT = 7.4$  mG/K), while the other hfs were independent of temperatures. Magnitudes and temperature dependence of the hfs suggest that the acetoxyl group eclipses the singly occupied orbital in the preferred rotational conformation of **9b**. This is actually a favorable conformation for the acyloxy migration.

(14) The rate of 1,2 (C → Si) acetoxy migration of **9b** is estimated as to be roughly  $10^{-10}$  s<sup>-1</sup> at -100 °C under reasonable assumptions. By use of a typical *A* factor for the radical rearrangement ( $\log A = 11-13$ ),<sup>16c</sup> the activation energy *E*<sub>a</sub> is calculated to be 7-9 kcal/mol, which is ca. 10 kcal/mol lower than that for the 1,2 (C → C) acyloxy rearrangement.<sup>10</sup> The very low *E*<sub>a</sub> may be mainly attributed to larger bond energy of Si-O than C-O.

(15) Recent ab initio MO calculations<sup>16</sup> for the migration showed that the barrier to the path leading to a dioxolanyl radical intermediate is much higher than the barrier for the direct migration via the polar cyclic transition state.<sup>16c,d</sup> The intermediacy of **10** during 1,2 (C → Si) acyloxy migration may suggest the substantial decrease of the barrier to the formation of the dioxolanyl radical by substitution of a silyl group.

(16) Saebo, S.; Beckwith, A. L. J.; Radom, L. *J. Am. Chem. Soc.* **1984**, *106*, 5119.

(17) In the strict sense of words as one referee has pointed out, we cannot exclude the possibility of other pathways to **4** and **5** without intervening **10**, because **10** was not detected. However, it is very difficult to postulate the proper mechanism other than the scheme shown to account for the formation of **4**. In connection to this point, we have observed an ESR spectrum of the  $\cdot\text{C}(\text{CH}_3)\text{SCH}_2\text{SiMe}_2\text{S}$  radical produced from  $\text{HSiMe}_2\text{CH}_2\text{SC}(\text{S})\text{CH}_3$  by hydrogen abstraction. Details will be published in a forthcoming paper.

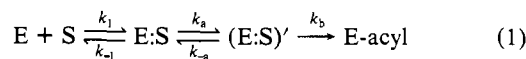
## Catalysis by Human Leukocyte Elastase. 5.<sup>1</sup> Structural Features of the Virtual Transition State for Acylation

Ross L. Stein

Pulmonary Pharmacology Section  
Department of Biomedical Research  
Stuart Pharmaceuticals  
a Division of ICI Americas Inc.  
Wilmington, Delaware 19897

Received July 5, 1985

Recent publications from this laboratory<sup>1,2</sup> suggest that HLE<sup>3</sup> is acylated according to the mechanism of eq 1 involving the



$$K_s = k_{-1}/k_1 \quad (2)$$

$$k_2 = \frac{k_a k_b}{k_{-a} + k_b} \quad (3)$$

$$k_E = k_2/K_s = \frac{k_1 k_a k_b}{k_{-1}(k_{-a} + k_b)} \quad (4)$$

intermediacy of a complex, (E:S)', formed from the Michaelis-complex through some physical process that is relatively insensitive to substrate structure and isotopic composition of the solvent. The rate-limiting step and transition-state properties of acylation depend on the relative magnitudes of  $k_{-a}$  and  $k_b$  (see eq 4). If  $k_{-a}$  and  $k_b$  are similar, the transition state of  $k_E$  will be "virtual"<sup>4,5</sup> and reflect properties of the transition states for both the physical step and the chemical steps of acylation.

It has also been suggested<sup>6,7</sup> that serine protease catalyzed reactions following the mechanism of eq 1 will generate proton inventories<sup>8</sup> of  $k_E$  that obey the relationship<sup>9</sup>

$$k_{E,n}/k_{E,n=0} = Z^n \left[ C_1 + \frac{C_2}{(1-n+\phi_T)^2} \right]^{-1} \quad (5)$$

where *Z* is a composite, transition-state fractionation factor reflecting the generalized solvent reorganization that occurs during substrate binding,  $\phi$  is one of two identical transition-state fractionation factors corresponding to the two exchangeable hydrogenic sites of the charge-relay system, and *C*<sub>1</sub> and *C*<sub>2</sub> are the transition-state contributions made by the physical and chemical steps, respectively. These transition-state contributions are expressed as

$$C_1 = k_E/k_a' \quad (6)$$

$$C_2 = k_E/k_b' \quad (7)$$

where  $k_a' = k_a/K_s$ ,  $k_b' = k_b/(K_s K_a)$ , and  $K_a = k_{-a}/k_a$ .<sup>4,5</sup> *Z* is similar in magnitude to solvent isotope effects on dissociation constants for complexes of serine proteases with their substrates or inhibitors and thus will frequently be greater than one.<sup>7</sup> This, combined with the fact that  $\phi_T$  values are invariably less than one<sup>2,8</sup> (typically,  $0.53 < \phi_T < 0.63$ ), allows us to predict that proton inventories of  $k_E$  will have a characteristic "bowed-upward" shape.<sup>8</sup>

(1) For part 4, see: Stein, R. L. *J. Am. Chem. Soc.* **1985**, *107*, 5767-5775.

(2) Stein, R. L. *J. Am. Chem. Soc.* **1983**, *105*, 5111-5116.

(3) Abbreviations: HLE, human leukocyte elastase; MeOSuc, *N*-methoxy-succinyl; pNA, *p*-nitroanilide; ONP, *p*-nitrophenyl ester.

(4) Schowen, R. L. In "Transition States of Biochemical Processes"; Gandour, R. D., Schowen, R. L., Eds.; Plenum Press: New York, 1978.

(5) Stein, R. L. *J. Org. Chem.* **1981**, *46*, 3328-3330.

(6) Stein, R. L.; Matta, M. S. *Fed. Proc.* **1985**, *44*, 1055.

(7) Stein, R. L. *J. Am. Chem. Soc.* **1985**, *107*, 6039-6042.

(8) Venkatasubban, K. S.; Schowen, R. L. *Crit. Rev. Biochem.* **1985**, *17*, 1-44.

(9) A derivation of eq 5 is provided in the supplementary material to this article.

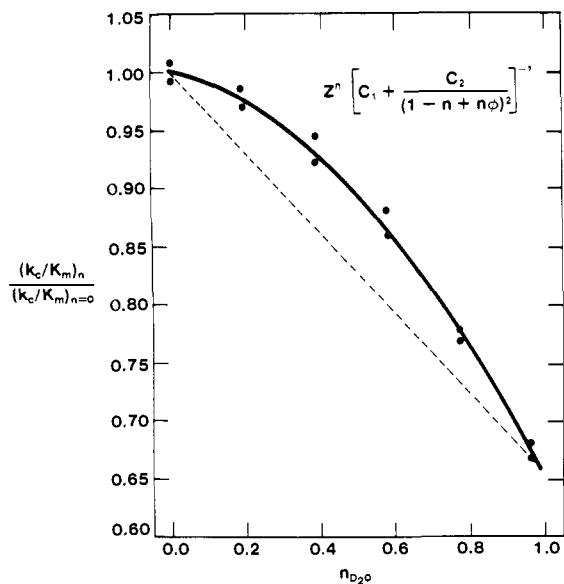


**Figure 1.** Proton inventory of  $k_E$  for the HLE-catalyzed hydrolysis of MeOSuc-Ala-Ala-Pro-Val-pNA. Values of  $k_E$  were determined as previously described.<sup>12</sup> The solid line passing through the data points was calculated from eq 5 and the parameters  $Z = 1.5$ ,  $\phi = 0.54$ ,  $C_1 = 0.46$ , and  $C_2 = 0.54$ . The dashed, straight line connects the points in pure light and heavy water.

To test the generality of the mechanism of eq 5, proton inventories of  $k_E$  were determined for the reaction of HLE with a series of peptide *p*-nitroanilide substrates<sup>10</sup> that span a 40-fold range of reactivity toward the enzyme: MeOSuc-Ala-Ala-Pro-Ala-pNA (I;  $k_E = 4500 \text{ M}^{-1} \text{ s}^{-1}$ ), MeOSuc-Ala-Ala-Pro-Ala-pNA (II;  $k_E = 27000 \text{ M}^{-1} \text{ s}^{-1}$ ), MeOSuc-Ala-Pro-Val-pNA (III;  $k_E = 56000 \text{ M}^{-1} \text{ s}^{-1}$ ), and MeOSuc-Ala-Ala-Pro-Val-pNA (IV;  $k_E = 182000 \text{ M}^{-1} \text{ s}^{-1}$ ).

All four proton inventories were bowed-upward, as illustrated in Figure 1 for MeOSuc-Ala-Ala-Pro-Val-pNA, and qualitatively confirm our expectations according to eq 5. The data sets were fit to this expression by nonlinear least squares with the parameter constraints<sup>7</sup> that  $Z = 1.5^7$  and  $\phi = 0.54$ .<sup>11</sup> The fits of the experimental data to eq 5 were all of excellent quality, similar to that of Figure 1, and thus support the generality of the mechanistic model implicit in this expression.<sup>6,7</sup>

The results of the curve-fitting procedures are given in Table I and clearly indicate that increases in substrate specificity, as reflected in  $k_E$ , are accompanied by significant changes in the structural features of the virtual transition state of  $k_E$ . These changes are indicated by substrate structural-dependent decreases in  $C_2$ , increases in  $C_1$ , and decreases in the (E:S)' partition ratio  $k_{-a}/k_b$ . Inspection of the  $k_a'$  and  $k_b'$  values of Table I reveals that the substrate structural-dependent change in the virtual transition-state structure is due predominantly to stabilization of the transition state of  $k_b$ . The magnitude of  $k_a$  is independent of substrate reactivity toward HLE (see Table I) and supports the view that the physical step of  $k_E$  is insensitive to substrate structure,<sup>1</sup> at least for tri- and tetrapeptide anilides. These  $k_a$  values are very similar to the value of  $k_2$  of  $200 \text{ s}^{-1}$  obtained by pre-steady-state kinetics for the HLE-catalyzed hydrolysis of MeOSuc-Ala-Ala-Pro-Val-ONP<sup>1</sup> and support an earlier argument<sup>1</sup> that  $k_2$  for this substrate equals  $k_a$ .

The ability of the mechanistic model of eq 5 to account for proton inventories of  $k_E$  for the four reactions of this study as well

**Table I.** Kinetics of HLE Acylation by Peptide *p*-Nitroanilide Substrates<sup>a</sup>

param	substrate			
	I	II	III	IV
$k_E^b$	$4.5 \pm 0.2$	$27 \pm 0.8$	$56 \pm 1.7$	$182 \pm 3.6$
$^D(k_E)$	$2.21 \pm 0.06$	$2.12 \pm 0.02$	$2.06 \pm 0.07$	$1.56 \pm 0.03$
$C_1^c$	$0.05 \pm 0.02$	$0.10 \pm 0.03$	$0.14 \pm 0.02$	$0.46 \pm 0.01$
$C_2^c$	$0.95 \pm 0.02$	$0.90 \pm 0.03$	$0.86 \pm 0.02$	$0.54 \pm 0.01$
$k_a'^d$	$90 \pm 54$	$270 \pm 24$	$400 \pm 58$	$400 \pm 12$
$k_b'^d$	$4.7 \pm 0.2$	$30 \pm 2$	$65 \pm 3$	$340 \pm 9$
$k_a^e$	$160 \pm 96$	$380 \pm 35$	$324 \pm 50$	$95 \pm 5$
$k_{-a}/k_b^f$	20	10	6	1.2

<sup>a</sup> Reaction conditions: 0.1 M HEPES, 0.5 M NaCl, pH 7.79 (and pD equivalent for solvent isotope effects and proton inventories), 3.3% Me<sub>2</sub>SO,  $25 \pm 0.1 \text{ }^\circ\text{C}$ . <sup>b</sup>  $k_E$ ,  $k_a'$ , and  $k_b'$  are expressed in units of  $\text{mM}^{-1} \text{ s}^{-1}$ , while  $k_a$  is in units of  $\text{s}^{-1}$ . <sup>c</sup> Values of  $C_1$  and  $C_2$  were determined by nonlinear least-squares fit of the dependence of  $k_E$  on mole fraction solvent deuterium,  $n$ , to eq 5 of the text.  $Z$  and  $\phi$  were constrained to 1.5 and 0.54, respectively. The proton inventories consisted of duplicate or triplicate  $k_E$  determinations at six values of  $n$  and were of the same general quality of the data shown in Figure 1. <sup>d</sup>  $k_a'$  and  $k_b'$  were calculated according to eq 6 and 7, respectively. <sup>e</sup>  $k_a = k_a'/K_s$ .  $K_s$  values I, 1.8 mM; II, 1.4 mM; III, 0.81 mM; IV, 0.24 mM.<sup>10</sup> <sup>f</sup>  $k_{-a}/k_b = C_1/C_2 = k_a'/k_b'$ .

as for several other protease-catalyzed reactions<sup>6-8</sup> supports the general importance of solvent reorganization in these associative processes and the existence of a virtual transition state whose properties are dependent on the structure of the substrate.

**Supplementary Material Available:** Derivation of eq 5 (3 pages). Ordering information is given on any current masthead page.

## Rhodopsin in Polymerized Bilayer Membranes

P. N. Tyminski, L. H. Latimer, and D. F. O'Brien\*

Research Laboratories, Eastman Kodak Co.  
Rochester, New York 14650

Received August 5, 1985

Rhodopsin (Rh), the major integral protein of the light-harvesting and energy-transducing portion of the rod cell,<sup>1</sup> can be reconstituted into phospholipid membrane bilayers with retention of its chemical regenerability,<sup>2</sup> photochemical functionality,<sup>3</sup> and ability to activate an enzyme cascade that results in the hydrolysis of  $>10^5$  cyclic GMP molecules per photon.<sup>4</sup> Current reports indicate that this enzyme cascade directly modulates the sodium permeability of the rod plasma membrane, which results in visual excitation.<sup>5</sup> We describe here the incorporation of Rh into partially polymerized bilayer membranes with retention of its chemical, photochemical, and enzymatic functionality. This functional protein behavior demonstrates that sensitive vertebrate membrane proteins can be usefully incorporated into membrane bilayers that have been modified by polymerization reactions.

Membrane bilayer-forming polymerizable amphiphiles introduced in recent years<sup>6</sup> include those with diacetylene,<sup>7-9</sup> meth-

(1) Reviewed by: O'Brien, D. F. *Science (Washington, D.C.)* **1982**, *218*, 961.

(2) Hong, K.; Hubbell, W. L. *Biochemistry* **1973**, *12*, 4517.

(3) O'Brien, D. F.; Costa, L. F.; Ott, R. A. *Biochemistry* **1977**, *16*, 1295.

O'Brien, D. F. *Methods Enzymol.* **1982**, *81*, 378.

(4) Tyminski, P. N.; O'Brien, D. F. *Biochemistry* **1984**, *23*, 3986.

(5) Fesenko, E. E.; Kolesnikov, S. S.; Lyubarsky, A. L. *Nature (London)* **1985**, *313*, 310. Nakatani, K.; Yau, K.-W. *Biophys. J.* **1985**, *47*, 356a.

(6) Reviewed by: O'Brien, D. F.; Klingbiel, R. T.; Specht, D. P.; Tyminski, P. N. *Ann. N. Y. Acad. Sci.* **1985**, *446*, 282.

(7) Johnston, D. S.; Sanghera, S.; Pons, M.; Chapman, D. *Biochim. Biophys. Acta* **1980**, *602*, 57.

(8) Hub, H. H.; Hupfer, B.; Koch, H.; Ringsdorf, H. *Angew. Chem., Int. Ed. Engl.* **1980**, *19*, 938.

(9) O'Brien, D. F.; Whitesides, T. H.; Klingbiel, R. T. *J. Polym. Sci., Polym. Lett. Ed.* **1981**, *19*, 95. Lopez, E.; O'Brien, D. F.; Whitesides, T. H. *J. Am. Chem. Soc.* **1982**, *104*, 305.

(10) Substrates were prepared by Drs. H. Hori and J. C. Powers (Georgia Institute of Technology). A complete kinetic characterization of the HLE-catalyzed hydrolyses of these and related substrates is underway as part of a collaboration with this laboratory.

(11) The use of the squared term in the proton inventory of eq 5 for all four substrates is justified by observations of simpler proton inventories of  $k_2$  for I<sup>10</sup> and  $k_3$  for III and IV.<sup>2,10</sup> These proton inventories are "bowed-downward" and are fit by the expression  $k_n/k_0 = (1 - n + n\phi)^2$ .

(12) Stein, R. L. *Arch. Biochem. Biophys.* **1985**, *236*, 677-680.